Pyridines with an Appended Metallocyclam Subunit. Versatile Building Blocks to Supramolecular Multielectron Redox Systems

Andrés De Blas,[1,2] Giancarlo De Santis,[1] Luigi Fabbrizzi,*[,1] Maurizio Licchelli,[1] Anna Maria Manotti Lanfredi,*[,3] Piersandro Pallavicini,[1] Antonio Poggi,[1] and Franco Ugozzoli[3]

Dipartimento di Chimica Generale, Università di Pavia, 27100 Pavia, Italy, and Istituto di Chimica Generale and Centro di Studio per la Strutturistica Diffrattometrica del CNR, Università di Parma, 43100 Parma, Italy

Received June 25, 1992

A pyridine subunit can be appended to a metallocyclam fragment through a template reaction which involves the condensation of a $[M^{II}(2,3,2\text{-tet})]^{2+}$ complex (M = Ni, Cu) with formaldehyde and pyridine-3-carboxamide or pyridine-4-carboxamide, in the presence of base. The crystal and molecular structure has been determined for the low-spin [3-(4-pyridiniumylcarbonyl)-1,3,5,8,12-pentaazacyclotetradecane]nickel(II), in which the nitrogen heteroatom of the pendant pyridine subunit is protonated. Single-crystal X-ray diffraction data were collected with the use of Cu Kα radiation: space group $P\bar{1}$ with a = 15.038 (2) Å, b = 13.576 (2) Å, c = 8.171 (2) Å, α = 108.12 (2)°, β = 84.66 (2)°, γ = 109.02 (2)°, V = 1498.8 (5) Å^3, and Z = 2 (R = 0.0751, R_w = 0.0751). Reaction of the metallocyclam–pyridine conjugates **3a,b** and **4a,b** ($M^{II}L^{2+}$) with $[Pt^{II}Cl_4]^{2-}$ and *cis*-$[Ru^{II}(bipy)_2Cl_2]$, in a 2:1 ratio, gives the *supercomplexes* *cis*-$[(M^{II}L)_2Pt^{II}Cl_2]^{4+}$ and *cis*-$[(M^{II}L)_2Ru^{II}(bipy)_2]^{6+}$, respectively. Cyclic voltammetry and controlled potential coulometry studies on nonaqueous solutions have shown that the *cis*-$[(Ni^{II}L)_2Pt^{II}Cl_2]^{4+}$ supercomplex undergoes a simultaneous two-electron oxidation to the *cis*-$[(Ni^{III}L)_2Pt^{II}Cl_2]^{6+}$ species, i.e. according to two one-electron processes, whose potentials are separated by the statistical term (36 mV). The *cis*-$[(M^{II}L)_2Ru^{II}(bipy)_2]^{6+}$ supercomplex, in acetonitrile solution 0.1 mol dm^{-3} in Bu_4NClO_4, undergoes a three-electron oxidation process: first, the one-electron oxidation of the Ru^{II} center, followed, at a potential 300 mV more positive, by the two-electron process involving the oxidation of the Ni^{II} ions of the macrocyclic subunits. On the other hand, in a 0.1 mol dm^{-3} Bu_3BzCl solution, the (1 + 2) sequence of the three-electron release of the *cis*-$[(M^{II}L)_2Ru^{II}(bipy)_2]^{6+}$ supercomplex is changed to (2 + 1): the oxidation of the two nickel centers occurs at a much lower potential, due to the stabilizing effect on Ni^{III} exerted by the axially bound Cl^- ions. Such a favorable effect is not experienced by the coordinatively saturated Ru^{II} center, which is oxidized at a potential 250 mV more positive.

Introduction

Two-electron redox chemistry is shown by a very limited number of metal-centered systems, i.e. those containing a p block metal. On the other hand, d metal centered systems typically display one-electron redox activity. An interesting property of d metal containing systems is that their redox behavior, due to the special nature of d orbitals, can be conveniently modulated by modifying the structural features of the coordinating framework wrapped around the metal center, a goal hardly achievable for non d metal centered systems. A rather obvious strategy to get two-electron systems based on d metal ions involves the covalent linking of two equivalent metal centered redox active subunits A, to give the dimeric system A–X–A, where X represents the segment linking the two equivalent subunits.

The covalent linking approach has been followed in the case of *metallocyclam* subunits, a type of redox-active fragment thoroughly investigated during the last two decades.[4] In fact, the incorporation of a metal center by a polyaza macrocycle promotes a rich redox chemistry, favoring access to unusual and otherwise unstable oxidation states.[5]

Among polyaza macrocycles of varying denticity and ring size, this behavior is especially evident in the case of the 14-membered tetraamine ligand *cyclam* (**1**), which forms the most stable macrocyclic complexes from both a thermodynamic and a kinetic point of view. Covalent linking of two cyclam subunits has

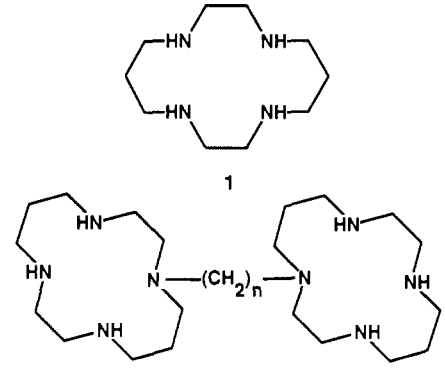

n = 2 : **2a**
n = 3 : **2b**
n = 4 : **2c**

produced a new class of binucleating ligands (biscyclams), which behave as ditopic receptors for transition metal ions, hosting for instance two equivalent redox-active metal ions.[6] In particular, it has been shown that dinickel(II) complexes with bismacrocycles of type **2** undergo a two-electron oxidation process through two consecutive one-electron processes, separated by the potential difference ΔE. As the length of the aliphatic chain $-(CH_2)_n-$ joining the two tetraamine rings increases, electrostatic repulsive effects between the adjacent metal centers decrease and ΔE decreases, too. For n = 3, ΔE reaches the limiting value of 36 mV, indicating that electrostatic effects have vanished, the redox

(1) Università di Pavia.
(2) Present address: Departamento de Química Pura y Aplicada, Universidad de Vigo, Vigo, Spain.
(3) Università di Parma.
(4) Lindoy, L. F. *The Chemistry of Macrocyclic Ligand Complexes*; Cambridge University Press: Cambridge, U.K., 1989.
(5) Fabbrizzi, L. *Comments Inorg. Chem.* **1985**, *4*, 33.
(6) Ciampolini, M.; Fabbrizzi, L.; Perotti, A.; Poggi, A.; Seghi, B.; Zanobini, F. *Inorg. Chem.* **1987**, *26*, 3527.

0020-1669/93/1332-0106$04.00/0

process is statistically controlled, and the two metal centers display independent redox behavior, through the Ni^{II}/Ni^{III} change.

We are now exploring a different approach to the synthesis of two-center redox systems, in which the redox fragments are held together not by covalent bonds but through coordinative interactions. The coordinative approach to the design of two-center systems displaying two-electron activity is described by the following equations:

$$L + A = L\text{–}A \quad (1)$$

$$M + 2L\text{–}A = [M(L\text{–}A)_2] \quad (2)$$

First, according to reaction 1, the redox-active fragment A is appended to a molecule L, possessing well-defined coordinating tendencies. Then, according to reaction 2, two (but even more, if required) molecules of the conjugate system L–A are coordinatively bound to a metal center M, to form the *supercomplex* $[M(L\text{–}A)_2]$.

The metal center M may be redox inactive, thus playing a purely architectural role, and the redox activity is located on and limited to the appended A fragments. However, the metal center may also display its own redox activity. In this case, the $[M(L\text{–}A)_2]$ supercomplex will present a richer multielectron redox activity located on both A and M. It is important that M–L coordinative bonds are stable from both a thermodynamic and a kinetic point of view. Moreover, their stability should not be altered by the redox changes taking place on the proximate subunits A and, in particular, by a change of the oxidation state of M, when occurring.

The *coordinative approach* to multielectron redox systems has been explored in this work by appending a *metallocyclam* subunit to the *pyridine* framework. Pyridine is one of the most traditional and versatile ligands of coordination chemistry, which forms especially stable complexes with d block metals. We have appended a metallocyclam subunit to pyridine through a novel metal template procedure which involves the one-pot condensation of the amides of 3- and 4-pyridinecarboxylic acids (nicotinic and isonicotinic acids, respectively) with formaldehyde and the Ni^{II} complex with the appropriate open-chain tetraamine. In particular, molecular systems **3** and **4** have been obtained. Then, the

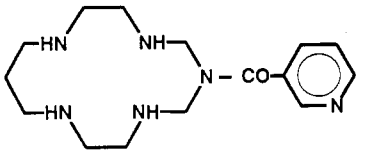

3

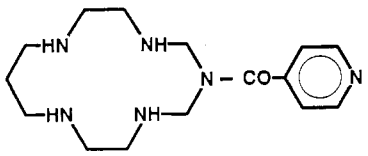

4

following fragments have been used as architectural elements: *cis*-$[Pt^{II}Cl_2]<$ and *cis*-$[Ru^{II}(bipy)_2]<$ (bipy = 2,2′-bipyridine). Pt^{II} and Ru^{II} metal centers form very stable coordinative bonds with the pyridine heteroatom from both a thermodynamic and kinetic point of view. In particular, Pt^{II}, which in the *cis*-$Pt^{II}Cl_2$ fragment does not display any redox activity, plays a merely structural role in the two-electron redox-active *cis*-$[Pt^{II}Cl_2(\mathbf{3})_2]^{4+}$ and *cis*-$[Pt^{II}Cl_2(\mathbf{4})_2]^{4+}$ complexes. On the other hand, the ruthenium center in the *cis*-$Ru^{II}(bipy)_2$ fragment is typically redox active through the Ru^{II}/Ru^{III} couple: thus, the *cis*-$[Ru^{II}(bipy)_2(\mathbf{3})_2]^{6+}$ and $[Ru^{II}(bipy)_2(\mathbf{4})_2]^{6+}$ supercomplexes display (2 + 1)-electron redox activity.

Assembled systems in which several subunits are linked together through noncovalent interactions have been defined as *supramolecular* systems.[7] In this sense, coordinatively linked multicenter systems belong to the realm of supramolecular chemistry and, in particular, they should be defined as *supramolecular coordination compounds* (or *supercomplexes*). Thus, the metallocyclam-substituted pyridines **3** and **4** can be considered as very convenient and versatile building blocks to supramolecular systems able to display multielectron redox activity. The aim of this work is to demonstrate that the coordinative approach is an especially easy and comfortable way to *supramolecular redox chemistry*.

Experimental Section

UV–visible spectra were measured on a Hewlett-Packard 8452A diode array spectrophotometer or on a Varian Cary 2300 spectrophotometer.

1,9-Diamino-3,7-diazanonane (2,3,2-tet) was prepared according to the procedure described for the synthesis of the homologous tetraamine 3,2,3-tet,[8] distilled at reduced pressure (125 °C; 5×10^{-2} Torr) and stored over NaOH in the refrigerator. Benzamide (Aldrich), pyridine-3-carboxamide (nicotinamide, Fluka), and pyridine-4-carboxamide (isonicotinamide, Fluka) were used without further purification. *cis*-$[Ru^{II}(2,2'\text{-bipyridine})_2Cl_2]$, $[Ru(bipy)_2Cl_2]$, was prepared as described.[9]

Synthesis of Macrocyclic Complexes. [3-Benzoyl-1,3,5,8,12-pentaazacyclotetradecane]copper(II) Nitrate [8a$(NO_3)_2$]. $Cu(NO_3)_2{\cdot}3H_2O$ (2.4 g, 10 mmol) was dissolved in ethanol (40 cm^3) in a three-neck round-bottomed flask equipped with reflux condenser, thermometer, and dropping funnel. A solution of 2,3,2-tet (1.6 g, 10 mmol) in ethanol (20 cm^3) was added dropwise to the magnetically stirred solution of copper nitrate. The resulting violet suspension was warmed to 50 °C, and benzamide (1.21 g, 10 mmol in 100 cm^3 of ethanol), triethylamine (1.5 cm^3, in one portion), and 40% aqueous formaldehyde (5 cm^3, in several portions during the reaction) were added through the dropping funnel. Heating and magnetic stirring were continued for 4 days. The violet precipitate formed after cooling to room temperature was filtered out on a sintered glass funnel, washed with acetone, and dried in vacuo. Yield: 45%. Anal. Calcd for $C_{16}H_{27}CuN_7O_7$: C, 39.16; H, 5.11; N, 19.97. Found: C, 38.93; H, 5.17; N, 19.77. Electronic spectrum (in aqueous 1 M HCl): λ_{max} 520 nm (ϵ = 89.3 $dm^3\ mol^{-1}\ cm^{-1}$).

[3-(3-Pyridiniumylcarbonyl)-1,3,5,8,12-pentaazacyclotetradecane]copper(II) Perchlorate [3a$(ClO_4)_2{\cdot}HClO_4$]. The synthesis was performed as in the case of complex **8a**. Pyridine-3-carboxamide (1.21 g, 10 mmol) was dissolved in 50 cm^3 of ethanol. After 5 days, the solution was concentrated and treated with 70% aqueous $HClO_4$. The pink-violet precipitate was filtered out and washed with cold ethanol and acetone. Yield: 33.4%. Anal. Calcd for $C_{15}H_{27}Cl_3CuN_6O_{13}$: C, 26.92; H, 4.04; N, 12.56. Found: C, 27.12; H, 4.09; N, 12.37. Electronic spectrum (in aqueous 1 M HCl): λ_{max} 520 nm (ϵ = 93.8 $dm^3\ mol^{-1}\ cm^{-1}$).

[3-(4-Pyridiniumylcarbonyl)-1,3,5,8,12-pentaazacyclotetradecane]copper(II) Perchlorate [4a$(ClO_4)_2{\cdot}HClO_4$]. The complex was prepared as described for complex **3a**. The locking fragment was in this case pyridine-4-carboxamide. Yield: 30%. Anal. Calcd for $C_{15}H_{27}Cl_3CuN_6O_{13}$: C, 26.92; H, 4.04; N, 12.56. Found: C, 26.72; H, 4.13; N, 12.43. Electronic spectrum (in aqueous 1 M HCl): λ_{max} 520 nm (ϵ = 94.1 $dm^3\ mol^{-1}\ cm^{-1}$).

[3-(Benzoyl)-1,3,5,8,12-pentaazacyclotetradecane]nickel(II) Perchlorate [8b$(ClO_4)_2$]. An ethanolic solution (10 cm^3) of 2,3,2-tet (1.6 g, 10 mmol) was slowly added under magnetic stirring to an ethanolic solution of $NiCl_2{\cdot}6H_2O$ (10 mmol in 40 cm^3) in a round-bottom flask (equipped as described for the synthesis of **8a**). The resulting blue solution was heated at 60 °C, and then benzamide (1.21 g, 10 mmol in 50 cm^3 of ethanol), triethylamine (1.5 cm^3), and 40% aqueous formaldehyde (10 cm^3, in several portions) were added. After 2 days, the pink solution was concentrated and treated with 70% aqueous $HClO_4$. A gummy yellow-orange precipitate immediately formed, which slowly solidified after some washings with diethyl ether. Yield: 14%. Anal. Calcd for $C_{16}H_{27}Cl_2N_5NiO_9$: C, 34.14; H, 4.83; N, 12.43. Found: C, 33.92; H, 4.71; N, 12.21.

(7) Lehn, J.-M. *Angew. Chem., Int. Ed. Engl.* **1988**, *27*, 89.
(8) Barefield, E. K.; Wagner, F.; Herlinger, A. W.; Dahl, A. R. *Inorg. Synth.* **1976**, *16*, 220.
(9) Sullivan, B. P.; Salmon, D. J.; Meyer, T. J. *Inorg. Chem.* **1978**, *17*, 3334.

[3-(3-Pyridiniumylcarbonyl)-1,3,5,8,12-pentaazacyclotetradecane]-nickel(II) Perchlorate [3b(ClO$_4$)$_2$·HClO$_4$]. The synthesis was performed as in the case of complex **8b**. The locking fragment was in this case pyridine-3-carboxamide. After 5 days, the solution was concentrated and treated with 70% aqueous HClO$_4$. A pink-violet precipitate formed, which was filtered out and washed with cold ethanol and acetone. Yield: 33%. Anal. Calcd for $C_{15}H_{27}Cl_3N_6NiO_{13}$: C, 27.12; H, 4.07; N, 12.64. Found: C, 27.39; H, 4.19; N, 12.50.

[3-(4-Pyridiniumylcarbonyl)-1,3,5,8,12-pentaazacyclotetradecane]-nickel(II) Perchlorate [4b(ClO$_4$)$_2$·HClO$_4$]. The complex was prepared as described for complex **3b**. The locking fragment was in this case pyridine-4-carboxamide. Yield: 30%. Anal. Calcd for $C_{15}H_{27}Cl_3N_6NiO_{13}$: C, 27.12; H, 4.07; N, 12.64. Found: C, 27.46; H, 4.24; N, 12.27.

Synthesis of Platinum(II) Supercomplexes. ***cis*-[Pt^{II}(3a)$_2$Cl$_2$](PtCl$_4$)(ClO$_4$)$_2$.** An aqueous solution of K_2PtCl_4 (50 mg, 0.12 mmol in 10 cm^3) was added dropwise to a solution of **3a**(ClO$_4$)$_2$·HClO$_4$ (160 mg, 0.24 mmol) in 10 cm^3 of a 1:1 DMSO/water solution. The mixture was magnetically stirred overnight; a solid formed, which was isolated by filtration and washed with water, ethanol, and diethyl ether. Yield: 21%. Anal. Calcd for $C_{30}H_{52}Cl_8N_{12}Ni_2O_{10}Pt_2$: C, 23.51; H, 3.40; N, 10.97. Found: C, 23.63; H, 3.47; N, 10.83.

***cis*-[Pt^{II}(4a)$_2$Cl$_2$](PtCl$_4$)(ClO$_4$)$_2$.** The synthesis was performed as in the case of the above mentioned platinum(II)–copper(II) supercomplex, but **4a**(ClO$_4$)$_2$·HClO$_4$ was used. Yield: 50%. Anal. Calcd for $C_{30}H_{52}Cl_8Cu_2N_{12}O_{10}Pt_2$: C, 23.36; H, 3.37; N, 10.90. Found: C, 23.31; H, 3.46; N, 11.10.

***cis*-[Pt^{II}(3b)$_2$Cl$_2$](PtCl$_4$)(ClO$_4$)$_2$.** A solution of K_2PtCl_4 (65 mg, 0.16 mmol) in water (10 cm^3) was very slowly added to a solution of **3b**(ClO$_4$)$_2$·HClO$_4$ (159 mg, 0.24 mmol) in water (10 cm^3). The mixture was magnetically stirred overnight; the precipitate was isolated by filtration and washed with water, ethanol, and diethyl ether. Yield: 70%. Anal. Calcd for $C_{30}H_{52}Cl_8N_{12}Ni_2O_{10}Pt_2$: C, 23.51; H, 3.40; N, 10.97. Found: C, 23.77; H, 3.50; N, 11.06.

***cis*-[Pt^{II}(4b)$_2$Cl$_2$](PtCl$_4$)(ClO$_4$)$_2$.** The synthesis was performed as in the case of the above mentioned platinum(II)–nickel(II) supercomplex, but **4b**(ClO$_4$)$_2$·HClO$_4$ was used. Yield: 69%. Anal. Calcd for $C_{30}H_{52}Cl_8N_{12}Ni_2O_{10}Pt_2$: C, 23.51; H, 3.40; N, 10.97. Found: C, 23.43; H, 3.49; N, 10.79.

Synthesis of Ruthenium(II) Supercomplexes. ***cis*-[Ru^{II}(4a)$_2$(bipy)$_2$}-(ClO$_4$)$_6$.** A solution of Ru(bipy)$_2$Cl$_2$ (104 mg, 0.187 mmol) in a water/ethanol mixture (10 cm^3, 1:1) was added to a 1:1 water/ethanol solution of **4a**(ClO$_4$)$_2$·HClO$_4$ (267.4 mg, 0.4 mmol, in 10 cm^3). The reaction mixture was refluxed for 4 h and then cooled to room temperature. A precipitate was obtained by addition of a saturated ethanolic solution of NaClO$_4$. The solid was filtered off, washed with small amounts of cold ethanol, and dried in vacuo. Yield: 43%. Anal. Calcd for $C_{50}H_{68}Cl_6Cu_2N_{16}O_{26}Ru$: C, 34.32; H, 3.91; N, 12.81. Found: C, 34.63; H, 3.94; N, 12.67.

***cis*-[Ru^{II}(4b)$_2$(bipy)$_2$}(ClO$_4$)$_6$.** The ruthenium(II)–dinickel(II) supercomplex was prepared by using the same experimental conditions given for the ruthenium(II)–dicopper(II) supercomplex. In this case, a hygroscopic product was isolated, whose analysis corresponds to the *trihydrate* salt. Yield: 64%. Anal. Calcd for $C_{50}H_{74}Cl_6N_{16}Ni_2O_{29}Ru$: C, 33.46; H, 4.13; N, 12.49. Found: C, 33.28; H, 4.11; N, 12.65.

Caution! Perchlorate salts of metal complexes are *potentially explosive*, and due care must be employed when handling them. In particular, such compounds should never be heated as solids.

Crystal Structure Determination. Single-crystal X-ray diffraction measurements were performed at 298 K, using Cu Kα radiation (λ = 1.541 78 Å) on a Siemens AED diffractometer on line on an IBM PC. Crystal data and the most relevant parameters used in the data collection and in the structure refinement are reported in Table I.

The cell parameters were determined by least-squares fit of 30 $(\theta, \chi, \phi)_{h,k,l}$ reflections in the range of $17.2 \leq \theta \leq 34.99°$ found in a random search of the reciprocal lattice. The intensities were determined by profile analysis, according to the method of Lehman and Larsen.[10] One standard reflection (−4,3,1) was measured every 100 collected ones, in order to check the crystal decay and the instrumental linearity. No significant fluctuations were observed. The reflections were corrected for Lorentz and polarization effects. Any attempt to solve the structure by automatic Patterson methods failed. The structure was solved by direct methods using the SIR88 computer program,[11] which showed the coordinates of Ni and Cl atoms. The structure was completed by Fourier methods and then refined with isotropic temperature factors by full-matrix least-squares methods using the SHELX package of computer programs.[12] At this stage two of the three ClO$_4^-$ anions showed disorder of the oxygen atoms. For the first anion the disorder was solved by taking the chlorine atom and one oxygen atom in common between two different orientations of the ClO$_4^-$ ion with occupancy factors of 0.7 and 0.3, respectively. The disorder of the second anion was solved in two different orientations of the oxygen atoms, with occupancy factors of 0.5.

Table I. Experimental Data for the X-ray Diffraction Studies

formula	$C_{15}H_{27}Cl_3N_6NiO_{13}$
cryst syst	triclinic
space group	$P\bar{1}$
cell dimens	
a, Å	15.038 (2)
b, Å	13.576 (2)
c, Å	8.171 (2)
α, deg	108.12 (2)
β, deg	84.66 (2)
γ, deg	109.02 (2)
V, Å^3	1498.8 (5)
Z	2
D_{calcd}, g cm^{-3}	1.472
F(000)	684
mol wt	664.48
linear abs coeff, cm^{-1}	40.209
diffractometer	Siemens AED
scan type	$\theta/2\theta$
scan speed, deg/min	3–12
scan width, deg	$(\theta - 0.65)$, $[\theta + (0.65 + \Delta\lambda\cdot\lambda^{-1}) \tan\theta]$
radiation (λ, Å)	Cu Kα (1.541 78)
2θ range, deg	6–140
reflcns measd	$\pm h, \pm k, l$
tot. no. of data measd	6108
criterion for obsn	$I_{hkl} \geq 2\sigma(I)$
no. of obsd data measd	3606
no. of unique obsd data	3326
no. of variables	399
final R	0.0751
final R_w	0.0751 (unit weights)

In the last stages of the refinement, anisotropic temperature factors were assigned to all the non-hydrogen atoms with the exception of the oxygen atoms of the two disordered ClO$_4^-$ anions. The hydrogen atoms of the N atoms of the polyaza macrocycle as well as the H atom bound to the pyridine heteroatom were located from the Fourier ΔF map and included in the refinement. The remaining ones were calculated with the geometrical constraint C–H = 1.08 Å and refined "riding" on their C atoms. The refinement was stopped at R = 0.071 (unit weights), and the highest residual peak in the final Fourier ΔF map was 0.89 e Å^{-3}. Final atomic coordinates for the non-hydrogen atoms are given in Table II.

The atomic scattering factors were obtained by analytical approximation.[13] Geometrical calculations were performed using PARST,[14] and the drawings were obtained by ORTEP (Figure 1) and PLUTO (Figure 2).[15] All the calculations were carried out on the Gould Encore 91 computer of the "Centro di Studio per la Strutturistica Diffrattometrica CNR", Parma, Italy, and on the CRAY Y-MP8/432 computer of the "Consorzio del Centro di Calcolo Elettronico Interuniversitario dell'Italia Nord-orientale" (CINECA), Casalecchio, Bologna, Italy.

Electrochemistry. The solvents used in the electrochemical experiments (MeCN and DMSO) were distilled over CaH_2 and stored under nitrogen over molecular sieves. Acetone was dried over molecular sieves overnight prior to use. Supporting electrolytes, [Bu$_4$N]ClO$_4$ (Fluka, polarographic grade) and [BzBu$_3$]NCl (Fluka), were used without further purification. Electrochemical measurements (cyclic voltammetry, CV, and differential pulse voltammetry, DPV) were performed in a conventional three-electrode cell, using a PAR 273 potentiostat/galvanostat, controlled by an IBM AT personal computer and driven by dedicated software. The working

(10) Lehman, M. S.; Larsen, F. K. *Acta Crystallogr., Sect. A* **1974**, *30*, 580.

(11) SIR88. Burla, M. C.; Camalli, M.; Cascarano, G.; Giacovazzo, C.; Polidori, G.; Spagna, R.; Viterbo, D. *J. Appl. Crystallogr.* **1989**, *22*, 389.

(12) Sheldrick, G. M. *SHELX76, System of Computing Programs*; University of Cambridge: Cambridge, U.K., 1976.

(13) *International Tables for X-ray Crystallography*; Kynoch Press: Birmingham, U.K., 1974; Vol. IV.

(14) Nardelli, M. *Comput. Chem.* **1983**, *7*, 95.

(15) ORTEP and PLUTO in CRYSRULER: Rizzoli, C.; Sangermano, V.; Calestani, G.; Andreetti, D. G. *J. Appl. Crystallogr.* **1987**, *20*, 436.

Table II. Fractional Atomic Coordinates ($\times 10^4$) and Equivalent Isotropic Thermal Parameters ($Å^2 \times 10^4$) with Esd's in Parentheses for the Non-Hydrogen Atoms of **4b**$(ClO_4)_2 \cdot HClO_4$

	x/a	y/b	z/c	U_{eq}[a]
Ni	2681 (1)	5633 (1)	8057 (2)	428 (6)
N(1)	3674 (5)	7866 (5)	7015 (9)	489 (30)
C(2)	4077 (7)	7850 (7)	8541 (11)	545 (38)
N(3)	3933 (4)	6689 (5)	8480 (7)	412 (29)
C(4)	4318 (6)	6668 (8)	10077 (11)	548 (40)
C(5)	4059 (6)	5482 (8)	9938 (12)	586 (46)
N(6)	3029 (5)	4990 (6)	9618 (9)	467 (28)
C(7)	2771 (8)	3782 (8)	9149 (13)	639 (46)
C(8)	1719 (7)	3257 (9)	8919 (14)	712 (52)
C(9)	1335 (7)	3393 (8)	7382 (15)	678 (54)
N(10)	1443 (5)	4575 (6)	7664 (10)	493 (31)
C(11)	971 (7)	4681 (9)	6217 (13)	631 (48)
C(12)	1258 (6)	5900 (9)	6443 (13)	610 (49)
N(13)	2311 (4)	6287 (6)	6529 (9)	464 (31)
C(14)	2666 (6)	7488 (7)	6903 (12)	520 (38)
C(15)	4194 (7)	8119 (7)	5666 (12)	524 (38)
C(16)	5226 (6)	8602 (7)	5885 (10)	490 (39)
C(17)	5799 (8)	7926 (9)	5357 (15)	729 (53)
C(18)	6758 (8)	8418 (9)	5484 (16)	803 (56)
N(19)	7130 (6)	9477 (7)	6097 (11)	658 (40)
C(20)	6601 (7)	10137 (8)	6606 (13)	662 (41)
C(21)	5650 (7)	9712 (7)	6511 (12)	589 (43)
O(22)	3833 (5)	8011 (6)	4299 (8)	699 (35)
Cl(1)	1453 (2)	6702 (2)	11894 (3)	574 (9)
Cl(2)	3627 (2)	4516 (2)	4001 (3)	517 (9)
Cl(3)	6892 (2)	9395 (2)	1032 (4)	872 (15)
O(1)	1256 (5)	7433 (6)	13458 (8)	768 (31)
O(2)	2207 (5)	7239 (6)	10998 (9)	758 (35)
O(3)	641 (5)	6172 (7)	10821 (10)	1040 (42)
O(4)	1719 (7)	5892 (7)	12336 (11)	1134 (51)
O(5)	4149 (5)	3940 (6)	2755 (8)	702 (32)
O(6)	3422 (7)	4163 (8)	5478 (13)	615 (28)
O(7)	4243 (8)	5672 (9)	4520 (14)	757 (32)
O(8)	2780 (8)	4465 (10)	3315 (15)	814 (33)
O(6′)	2671 (16)	3939 (21)	3528 (30)	684 (64)
O(7′)	3804 (14)	4444 (16)	5729 (25)	424 (47)
O(8′)	3863 (15)	5647 (16)	4218 (25)	452 (49)
O(9)	7684 (11)	9822 (19)	−33 (23)	2523 (138)
O(10)	7112 (12)	10087 (13)	2807 (13)	1328 (72)
O(11)	6808 (17)	8288 (9)	910 (30)	2667 (167)
O(12)	6053 (9)	9482 (15)	447 (22)	1348 (72)
O(13)	7268 (15)	10334 (11)	375 (25)	1422 (89)
O(14)	6080 (12)	9443 (17)	2076 (26)	1958 (113)
O(15)	6660 (16)	8414 (12)	−465 (20)	1900 (113)
O(16)	7636 (13)	9348 (21)	2018 (31)	1956 (106)

[a] Equivalent isotropic U defined as one-third of the trace of the orthogonalized U_{ij} tensor.

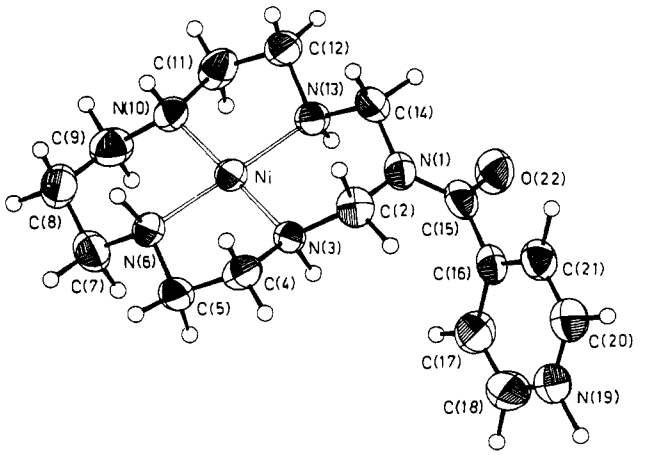

Figure 1. ORTEP drawing of the [3-(4-pyridiniumylcarbonyl)-1,3,5,8,12-pentaazacyclotetradecane]nickel(II) ion (**4b**).

electrode was a platinum microsphere, and the counter electrode was a platinum foil. A silver wire was used as a pseudoreference electrode and was calibrated using ferrocene as an internal standard. Thus, all the potentials reported in this work have been referred to the classical $Fc^+/$

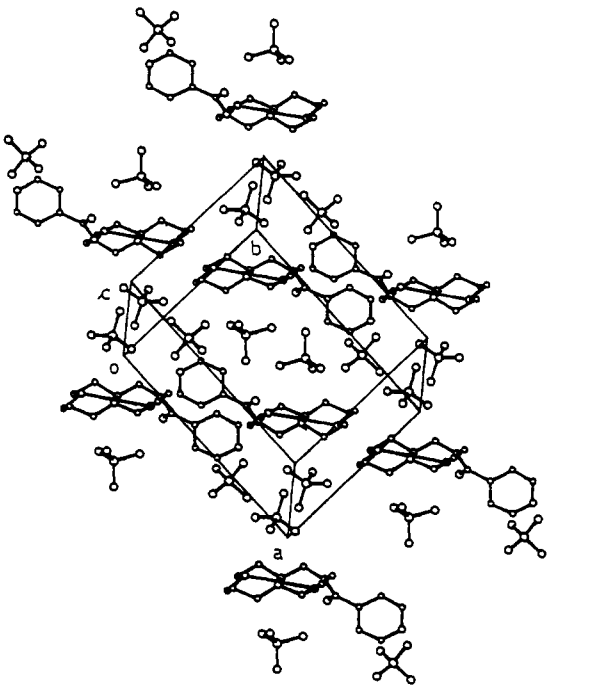

Figure 2. Molecular packing of the [3-(4-pyridiniumylcarbonyl)-1,3,5,8,12-pentaazacyclotetradecane]nickel(II) perchlorate salt [**4b**-$(ClO_4)_2 \cdot HClO_4$].

Fc standard couple. Controlled potential coulometry experiments were performed on MeCN solutions (5×10^{-4}–10^{-3} mol dm^{-3}), employing a platinum gauze as a working electrode.

Results and Discussion

1. The Aryl Amide Group as a Locking Fragment in the Template Synthesis of Pentaaza Four-Coordinating Macrocycles. In one of the most classical reactions of macrocyclic chemistry, Sargeson used NH_3 and formaldehyde to cap the $[Co^{III}(en)_3]^{3+}$ complex and the sepulchrate complex **5** was obtained.[16] Some

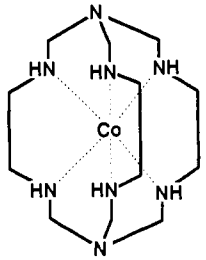

5

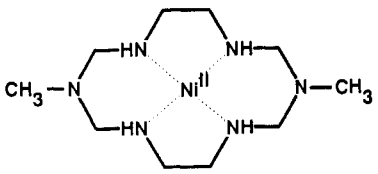

6

years later, Suh et al. converted Sargeson's tridimensional template synthesis to two dimensions and used a primary amine, RNH_2, and formaldehyde to close the $[Ni^{II}(en)_2]^{2+}$ complex and to give the hexaaza macrocyclic complex **6**.[17]

We recently carried out an analogous template reaction involving the open-chain tetraamine 2,3,2-tet, formaldehyde, and methylamine (see Scheme I) to give the low-spin pentaaza macrocyclic complex **7b**, $[Ni^{II}(azacyclam)](ClO_4)_2$.[18] X-ray investigation on **7b** showed that the tertiary nitrogen atom of the pentaaza macrocycle is not coordinated and that azacyclam displays coordinating tendencies (in terms of bond distances and angles) strictly similar to those of cyclam in analogous complexes.[18]

(16) Creaser, I. J.; Harrowfield, J. M.; Hertl, A. J.; Sargeson, A. M.; Springborg, J.; Geue, R. J.; Snow, M. R. *J. Am. Chem. Soc.* **1977**, *99*, 3181.
(17) Suh, M. P.; Kang, S. G. *Inorg. Chem.* **1988**, *27*, 2544.
(18) Fabbrizzi, L.; Manotti Lanfredi, A. M.; Pallavicini, P.; Perotti, A.; Taglietti, A.; Ugozzoli, F. *J. Chem. Soc., Dalton Trans.* **1991**, 3263.

Scheme I

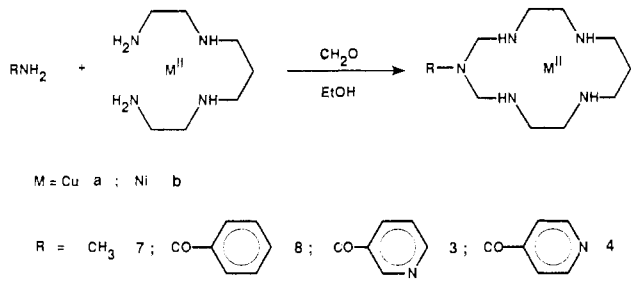

Moreover, the tertiary amine group appears as distinctly flattened, thus presenting a pronounced sp^2, rather than sp^3, character. This should drastically reduce its basicity. Indeed, the tertiary amine group presents extremely low basic tendencies and is protonated only in a strong acid solution of concentration 1 mol dm^{-3} or higher. This demonstrates that the fifth nitrogen atom introduced by template syntheses of the type described above exerts a purely structural function and does not alter the cyclam-like donor properties of the macrocycle. In any case, the $[Ni^{II}(azacyclam)]^{2+}$ complex, **7b**, displays the same distinctive solution properties as the corresponding $[Ni^{II}(cyclam)]^{2+}$ complex: (i) inertness toward demetalation and (ii) easy access to the Ni^{III} state.

The very crucial step of macrocycle formation should be the attack of the deprotonated primary amine on the $-N{=}CH_2$ imine bonds derived from the Schiff base condensation of the terminal $-NH_2$ groups of coordinated 2,3,2-tet with formaldehyde. This suggests that electron-withdrawing R groups, which make the attached $-NH_2$ group of the locking fragment more acidic, would favor cyclization.

In fact, we found that primary aryl amides can efficiently replace primary amines as *locking fragments* in the template synthesis of pentaaza four-coordinating rings (generally named azacyclams) and that both Ni^{II} and Cu^{II} ions work well as templating centers. In particular, reaction of a $[M^{II}(2,3,2\text{-tet})]^{2+}$ complex (M = Ni, Cu) with benzamide and excess formaldehyde, in an ethanolic solution containing 1 equiv of triethylamine, gives the corresponding pentaaza macrocyclic four-coordinated metal complexes **8a**,**8b**, as illustrated in Scheme I. Template ring closure works well also if benzamide is replaced by pyridine-3-carboxamide and pyridine-4-carboxamide (see Scheme I), and corresponding complexes **3a**,**b** and **4a**,**b** form. All the complexes persist in strongly acidic solutions. In particular, complexes of type **3** and **4** were isolated after addition of concentrated perchloric acid to the ethanolic reaction mixture as perchlorate salts, in which the heterocycle is present in the form of a pyridinium cation. Thus, elemental analyses correspond to the general formula $[M^{II}L](ClO_4)_2{\cdot}HClO_4$, where L indicates the azacyclam ring carrying a pendant pyridine subunit. In general (see details in the Experimental Section), reaction yields are higher for Cu^{II} than for Ni^{II} complexes and are slightly higher than observed for the corresponding reactions in which an alkylamine was used as a locking fragment. A detailed investigation of the mechanistic aspects of template reactions of the type involving RNH_2 groups (amines and amides of varying acidic nature) will be published elsewhere.[19] In particular, the $\mathbf{4b}(ClO_4)_2{\cdot}HClO_4$ (I) complex salt was obtained in orange crystals suitable for X-ray investigation. The molecular structure of I has definitively confirmed that the nitrogen atom of the amido group acted as a locking fragment of the macrocycle and is not involved in coordination to the Ni^{II} ion.

Crystal and Molecular Structure of $\mathbf{4b}(ClO_4)_2{\cdot}HClO_4$. The compound I contains discrete perchlorate anions and cationic complexes of formula $\{3\text{-}pyH^+[Ni^{II}L]^{2+}\}$. A view of the tripositive cation is given in Figure 1. Selected bond distances are reported in Table III.

Table III. Relevant Bond Distances (Å) and Angles (deg) of $\mathbf{4b}(ClO_4)_2{\cdot}HClO_4$

Distances			
Ni–N(3)	1.943 (5)	Ni–N(10)	1.927 (7)
Ni–N(6)	1.944 (9)	Ni–N(13)	1.949 (9)
N(1)–C(2)	1.445 (13)	N(13)–C(14)	1.480 (12)
C(2)–N(3)	1.505 (12)	C(14)–N(1)	1.435 (11)
N(3)–C(4)	1.488 (12)	N(1)–C(15)	1.358 (12)
C(4)–C(5)	1.498 (15)	C(15)–C(16)	1.479 (13)
C(5)–N(6)	1.485 (11)	C(16)–C(17)	1.404 (17)
N(6)–C(7)	1.486 (13)	C(17)–C(18)	1.376 (15)
C(7)–C(8)	1.511 (14)	C(18)–N(19)	1.308 (13)
C(8)–C(9)	1.514 (19)	N(19)–C(20)	1.334 (16)
C(9)–N(10)	1.504 (14)	C(20)–C(21)	1.356 (14)
N(10)–C(11)	1.500 (16)	C(21)–C(16)	1.376 (11)
C(11)–C(12)	1.523 (17)	C(15)–O(22)	1.234 (13)
C(12)–N(13)	1.498 (10)		
Angles			
N(3)–Ni–N(6)	86.5 (3)	N(10)–Ni–N(13)	86.9 (3)
N(6)–Ni–N(10)	92.6 (4)	N(13)–Ni–N(3)	94.0 (3)
N(6)–Ni–N(13)	178.7 (3)	N(10)–Ni–N(3)	179.1 (3)
C(2)–N(1)–C(14)	116.1 (7)	C(12)–N(13)–C(14)	109.9 (7)
N(1)–C(2)–N(3)	109.7 (7)	C(12)–N(13)–Ni	107.3 (6)
C(2)–N(3)–C(4)	109.9 (6)	C(14)–N(13)–Ni	118.6 (6)
C(2)–N(3)–Ni	119.5 (6)	N(13)–C(14)–Ni	110.2 (7)
C(4)–N(3)–Ni	108.5 (5)	C(14)–N(1)–C(15)	120.1 (8)
N(3)–C(4)–C(5)	104.9 (7)	C(15)–N(1)–C(2)	123.5 (8)
C(4)–C(5)–N(6)	107.9 (8)	N(1)–C(15)–O(22)	122.4 (9)
C(5)–N(6)–C(7)	109.5 (8)	N(1)–C(15)–C(16)	118.6 (8)
C(5)–N(6)–Ni	108.0 (6)	O(22)–C(15)–C(16)	118.9 (9)
C(7)–N(6)–Ni	118.8 (6)	C(15)–C(16)–C(21)	121.6 (9)
N(6)–C(7)–C(8)	110.9 (9)	C(15)–C(16)–C(17)	119.7 (9)
C(7)–C(8)–C(9)	113.3 (9)	C(17)–C(16)–C(21)	118.5 (9)
C(8)–C(9)–N(10)	110.2 (9)	C(16)–C(17)–C(18)	117.7 (10)
C(9)–N(10)–C(11)	109.5 (8)	C(17)–C(18)–N(19)	121.6 (12)
C(9)–N(10)–Ni	119.2 (6)	C(18)–N(19)–C(20)	121.8 (10)
C(11)–N(10)–Ni	109.4 (6)	N(19)–C(20)–C(21)	119.9 (10)
N(10)–C(11)–C(12)	105.7 (8)	C(20)–C(21)–C(16)	120.4 (9)
C(11)–C(12)–N(13)	105.3 (9)		
Relevant Intermolecular Hydrogen Bonds			
N(3)···O(7)	3.16 (1)	H(3)···O(7)	2.19 (1)
N(6)···O(4)	3.06 (1)	H(6)···O(4)	2.06 (3)
N(10)···O(3)	3.23 (1)	H(10)···O(3)	2.51 (4)
N(13)···O(8)	3.20 (1)	H(13)···O(8)	2.37 (5)
N(13)···O(8′)	3.04 (1)	H(13)···O(8′)	2.33 (7)
C(17)···O(7)	3.10 (1)	H(17)···O(7)	2.05 (3)
N(3)–H(3)–O(7)	148 (1)	N(13)–H(13)–O(8)	149 (3)
N(6)–H(6)–O(4)	151 (2)	N(13)–H(13)–O(8′)	133 (2)
N(10)–H(10)–O(3)	143 (3)	C(17)–H(17)–O(7)	151 (2)

In the tripositive complex cation, the Ni^{II} metal center is coplanarly chelated by the four secondary amine nitrogen atoms of the pentaaza macrocyclic subunit, according to a square stereochemistry. The Ni^{II} ion is displaced from the N_4 donor set least-squares plane by 0.01 Å. The Ni^{II}–N distances are those generally observed for low-spin tetraaza macrocyclic complexes.[20] One of the three perchlorate anions is strongly packed with the pyridinium ring. The other two perchlorate anions are accommodated on the two opposite sides with respect to the N_4 coordination plane, according to an axial arrangement. The shortest Ni^{II}–O distances [Ni–O(6) = 2.839 (10) Å and Ni^{II}–O(2) = 2.911 (7) Å] exclude any coordination of the metal center. However, the two perchlorate ions are hydrogen bonded to the complex cation through two pairs of hydrogen bonds, which involve the N–H groups of the coordinated secondary amine nitrogen atoms. In particular, two N–H groups point up and the other

(19) De Blas, A.; De Santis, G.; Fabbrizzi, L.; Licchelli, M.; Manotti Lanfredi, A. M.; Morosini, P.; Pallavicini, P.; Ugozzoli, F. Submitted for publication.

(20) Henrik, K.; Tasker, P. A.; Lindoy, L. F. *Prog. Inorg. Chem.* **1985**, *33*, 1.

Table IV. Half-Wave Potential Values (V) Associated with the Oxidation of Ni^{II} Complexes and Ni^{II}–Pt^{II} and Ni^{II}–Ru^{II} Supercomplexes[a]

	MeCN/$[Bu_4N]ClO_4$	MeCN/$[BzBu_3N]Cl$	DMSO/$[Bu_4N]ClO_4$	DMSO/$[BzBu_3N]Cl$
3b$(ClO_4)_2 \cdot HClO_4$	0.741	0.113	0.350	
4b$(ClO_4)_2 \cdot HClO_4$	0.752	0.115	0.351	
8b$(ClO_4)_2$	0.716			
$[Ru^{II}(bipy)_2(pyam)_2](ClO_4)_2$[b]	0.404	0.400[c]	0.365	
$[Ru^{II}(bipy)_2(\mathbf{4b})_2](ClO_4)_6$	0.440, 0.736 (E_1 = 0.718, E_2 = 0.754)[d]	0.083, 0.344 (E_1 = 0.065, E_2 = 0.101)[d]	0.380[e]	
$[Pt^{II}(\mathbf{3b})_2Cl_2](PtCl_4)(ClO_4)_2$	*f*	*f*		0.029 (E_1 = 0.011, E_2 = 0.047)[d]
$[Pt^{II}(\mathbf{4b})_2Cl_2](PtCl_4)(ClO_4)_2$	*f*	*f*		0.027 (E_1 = 0.009, E_2 = 0.045)[d]

[a] Electrochemical experiments were performed in selected media made 0.1 M in $[Bu_4N]ClO_4$ or in $[BzBu_3N]Cl$. $E_{1/2}$ values are referred to the ferrocenium/ferrocene (Fc^+/Fc) couple. [b] The complex was prepared according to ref 25 (pyam = pyridine-4-carboxamide). [c] The oxidation peak is partially hidden by Cl^- discharge. [d] The potential values E_1 and E_2 are referred to the processes involving each Ni(azacyclam) subunit in the supercomplex. As the two-electron process is statistically controlled ($E_2 - E_1$ = 36 mV, at 36 °C), it follows that $E_1 = E_{1/2} - 18$ mV and $E_2 = E_{1/2} + 18$ mV. [e] Three-electron oxidation peak. [f] The supercomplex is not soluble in MeCN.

two point down, with respect to the N_4 coordination plane (see the crystal packing shown in Figure 2). Such an intermolecular hydrogen-bonding system of axial symmetry has been previously observed with another Ni^{II} low-spin complex salt: $[Ni^{II}(ms$-5,7,12,14-tetramethyl-1,4,8,11-tetraazacyclotetradecane)]-$(ClO_4)_2$.[21] Also in this case, the ClO_4^- ions are too distant to interact with the metal center.

The geometrical parameters of the coordination sphere of Ni^{II} in I can be compared with those found for the corresponding low-spin Ni^{II} complex with the previously investigated azacyclam system, **7b**, $[Ni^{II}(azacyclam)](ClO_4)_2$ (II).[18] Ni–N distances are only slightly larger in I than in II (1.927(7)–1.949 (9) Å and 1.921 (6)–1.938 (6) Å, respectively). As observed in the azacyclam complex II, the bis(ethylenediamine)–nickel(II) moiety of I exhibits a λ–δ configuration, due to the existence of a pseudosymmetry plane, involving only the macrocyclic portion of the conjugate complex and bisecting the N(3)–Ni–N(13) and N(6)–Ni–N(10) bond angles.

In both complexes I and II, the five-membered rings present a *gauche* conformation and the six-membered ones a *chair* conformation. Moreover, whereas a noncentrosymmetrical crystal of II contained only molecules with an *RSRS* configuration of the four-coordinated nitrogen atoms, compound I, which crystallizes in a centrosymmetric space group, is a racemic mixture of *RSRS* and *SRSR* diastereoisomers.

The most striking differences of the macrocyclic frameworks present in I and II are observed in the portion involving the N(1)–C(15) group, which replaces the middle $-CH_2-$ group of one of the trimethylenic chains of the plain cyclam ring. In particular, the Ni–N(1) distance is substantially shorter in I than in II (3.250 (7) Å vs 3.319 (7) Å), indicating a contraction of the pseudo-cyclam ring. Such a contraction is not present in the opposite portion of the ring, the Ni–C(8) distances being almost coincident (3.343 (12) and 3.349 (10) Å, respectively). This difference seems to depend upon the nature of the N(1) atom, not involved in the coordination to the metal and expected to play a purely structural role. It has been previously observed that the $N(1)C_3$ group in complex II is rather flattened, its N–C distances are unusually short, and it can be protonated only in a strongly acidic solution: all this evidence leads to suggest that the N(1) atom in II does not have pure sp^3 character, but rather an intermediate hybridization between sp^3 and sp^2.[18] On the other hand, the N(1) atom in the presently investigated system belongs to an amido group and presents distinct sp^2 features: planarity of the NC_3 moiety and relatively short N–C bonds. In particular, the N(1)–C distances are substantially smaller in I than in II (average values 1.41 (1) and 1.45 (1) Å, respectively), which makes a portion of the pseudo-cyclam ring contract and the Ni^{II}–N(1) distance reduce.

To the best of our knowledge, supported by a systematic search on the Cambridge Crystallographic Data File, protonation of the isonicotinoyl fragment has not been structurally characterized until now. An interesting feature observed in the present structure is that the bulky 4-pyridyl moiety of the isonicotinoyl group is not coplanar but nearly orthogonal with respect to the plane of the carbonylamino fragment. In particular, the dihedral angle formed by the N(1)C(15)O(22) plane with the protonated pyridine ring is 88.5 (4)°. It is probable that such an orientation is further stabilized by intermolecular C–H···O hydrogen bonding, involving the pyridinic C(17) atom and the O(7) atom of the proximate perchlorate ion (see Table III). Notice that this perchlorate ion and the pyridinium ring lie on the same side with respect to the NiN_4 coordination plane. The geometric parameters for the isonicotinoyl group are as expected. Bond angles of the heteroatom N(19) favorably compare with those found, in other structures, for the pyridinium $>NH^+$ group.[22]

Solution Properties of the Aryl Amido–Azacyclam Complexes. Both Ni^{II} and Cu^{II} complexes, **8b** and **8a**, present the typical macrocyclic inertness toward demetalation, lasting for days in 1 mol dm^{-3} HCl solution, as monitored by the persistence of the corresponding d–d absorption band. Noticeably, the energies of the d–d bands are almost coincident with those observed for the corresponding cyclam complexes (Ni^{II}, 21 930 cm^{-1} for **8b**, 22 120 cm^{-1} for $[Ni^{II}(cyclam)]^{2+}$; Cu^{II}, 19 230 cm^{-1} for **8a**, 19 600 cm^{-1} for $[Cu^{II}(cyclam)]^{2+}$ in 1 M HCl solution), indicating that the 14-membered pentaaza macrocycle present in complexes of type **8** display the same coordinating tendencies as the original tetraaza macrocycle cyclam. In particular, the amido group, in analogy with that observed with the azacyclam complex, exerts a purely structural role, being not involved in the coordination of the encircled metal center. As far as the redox behavior is concerned, the Ni^{II} complex **8b** undergoes a reversible one-electron oxidation process at the platinum electrode in a MeCN solution made 0.1 mol dm^{-3} in Bu_4NClO_4, as shown by the cyclic voltammetry investigation ($E_{1/2}$ = 0.716 V vs Fc^+/Fc). This value is more positive than that observed for the Ni^{II}/Ni^{III} redox change in the reference *cyclam* system (0.590 V). This indicates that replacing a $-CH_2-$ group of the cyclam framework by an aryl amido group (**8b** system) should reduce, through an electron-withdrawing effect, the donor tendencies of the adjacent secondary amine group, making access to the Ni^{III} state more difficult.

The Ni^{II} complexes **3b** and **4b** undergo a one-electron oxidation process at a platinum working electrode in MeCN solution at potentials only slightly more positive than that measured for the reference benzamido–azacyclam complex **8b** (0.741 and 0.752 V vs Fc^+/Fc). The positive charge on the pyridine heteroatom does not seem to influence too seriously, through electrostatic repulsive effects, the 2+ to 3+ charge increase, taking place on the adjacent macrocyclic subunit. In any case, addition of stoichiometric NaOH, through a standard aqueous solution, to the MeCN

(21) Hay, R. W.; Jeragh, B.; Ferguson, G.; Kaitner, B.; Ruhl, B. L. *J. Chem. Soc., Dalton Trans.* **1982**, 1531.

(22) Belicchi Ferrari, M.; Fava Gasparri, G.; Lanfranchi, M.; Pelizzi, C.; Tarasconi, P. *J. Chem. Soc., Dalton Trans.* **1991**, 1951.

solutions makes the $E_{1/2}(Ni^{III}/Ni^{II})$ values of **3b** and **4b** decrease by 50–60 mV. All pertinent $E_{1/2}(Ni^{III}/Ni^{II})$ values are reported in Table IV.

All the above evidence indicates that the template synthetic procedure illustrated in Scheme I makes available pyridine ligands carrying an appended redox-active subunit. In particular, the attached polyaza macrocyclic complex behaves as the cyclam analogue and the Ni^{II} derivative is prone to oxidation to the Ni^{III} state.

2. Reaction of $[Pt^{II}Cl_4]^{2-}$ with the Pyridine–Metallocyclam Conjugates. Two chloride ions of the square $[Pt^{II}Cl_4]^{2-}$ complex can be easily replaced by pyridine ligands (py). Moreover, the trans-effect drives the reaction to the *cis*-$[Pt^{II}(py)_2Cl_2]$ complex.[23] Reaction of $[Pt^{II}Cl_4]^{2-}$ with 2 equiv of $[n\mathbf{a}(ClO_4)_2]\cdot HClO_4$ or $[n\mathbf{b}(ClO_4)_2]\cdot HClO_4$ ($n = 3, 4$) gives compounds whose C, H, and N analyses correspond to the formula $[Pt^{II}(n\mathbf{a})_2Cl_2][Pt^{II}Cl_4](ClO_4)_2$ and $[Pt^{II}(n\mathbf{b})_2Cl_2][PtCl_4](ClO_4)_2$. Also in this case, cis-derivatives should be formed. Unfortunately, we were not able to grow crystals suitable for X-ray investigations.

As far as the solution behavior is concerned, both *cis*-$[Pt^{II}(\mathbf{3b})_2Cl_2][Pt^{II}Cl_4](ClO_4)_2$ and *cis*-$[Pt^{II}(\mathbf{4b})_2Cl_2][Pt^{II}Cl_4](ClO_4)_2$ compounds are insoluble in water and in the most common organic solvents of varying polarity. However, they are moderately soluble (about 5×10^{-4} mol dm^{-3}) in DMSO, made 0.1 mol dm^{-3} in $BzBu_3Cl$, and electrochemical investigations were carried out in this medium. The DPV profile disclosed for both compounds a symmetric peak with a half-peak width of about 90 mV. The corresponding $E_{1/2}$ values are reported in Table IV. In the case of the *cis*-$[Pt^{II}(\mathbf{3b})_2Cl_2][Pt^{II}Cl_4](ClO_4)_2$ compound, a controlled potential coulometry experiment was carried out. The potential of the working platinum gauze was 150 mV higher than peak potential measured with the DPV experiment, and the integrated current curve indicated the consumption of 1.94 mol of electrons/mol of complex. These data suggest that each investigated compound undergoes a two-electron oxidation process at the platinum electrode, according to two consecutive one-electron reversible steps. In particular, each one-electron oxidation process should involve the Ni^{II}/Ni^{III} redox change which takes place inside each appended metallocyclam subunit, as described by the following equations:

$$cis\text{-}[Pt^{II}(n\text{-py}[Ni^{II}L]_2)Cl_2]^{4+} = cis\text{-}[Pt^{II}(n\text{-py}[Ni^{III}L])(n\text{-py}[Ni^{II}L])Cl_2]^{5+} + e^- \quad (3)$$

$$cis\text{-}[Pt^{II}(n\text{-py}[Ni^{III}L])(n\text{-py}[Ni^{II}L])Cl_2]^{5+} = cis\text{-}[Pt^{II}(n\text{-py}[Ni^{III}L]_2)Cl_2]^{6+} + e^- \quad (4)$$

The observed half-peak width in the DPV profile corresponds to a statistically controlled process, with an $(E_2 - E_1)$ potential difference of 36 mV.[24] This indicates that no electrostatic repulsion effects exist between the two appended rings and each metallocyclam subunit displays independent redox activity. In this sense, *cis*-$[Pt^{II}(\mathbf{3b})_2Cl_2]^{4+}$ and *cis*-$[Pt^{II}(\mathbf{4b})_2Cl_2]^{4+}$ supercomplexes behave in the same way as the dinickel(II) complex of the biscyclam ligand in which the two tetraaza rings are joined by a $-(CH_2)_3-$ segment.[6] Both systems, biscyclam and Pt^{II}-linked azacyclam dinickel(II) complexes, release two electrons according to a statistically controlled process.

3. Reaction of *cis*-$[Ru^{II}(bipy)_2Cl_2]$ with the Pyridine–Metallocyclam Conjugates. It is well-known that in the *cis*-$[Ru^{II}(bipy)_2Cl_2]$ complex (bipy = 2,2′-bipyridine) the two chloride ions can easily be replaced by nitrogeneous ligands,[25] to give a very stable species from both a thermodynamic and a kinetic point of view.

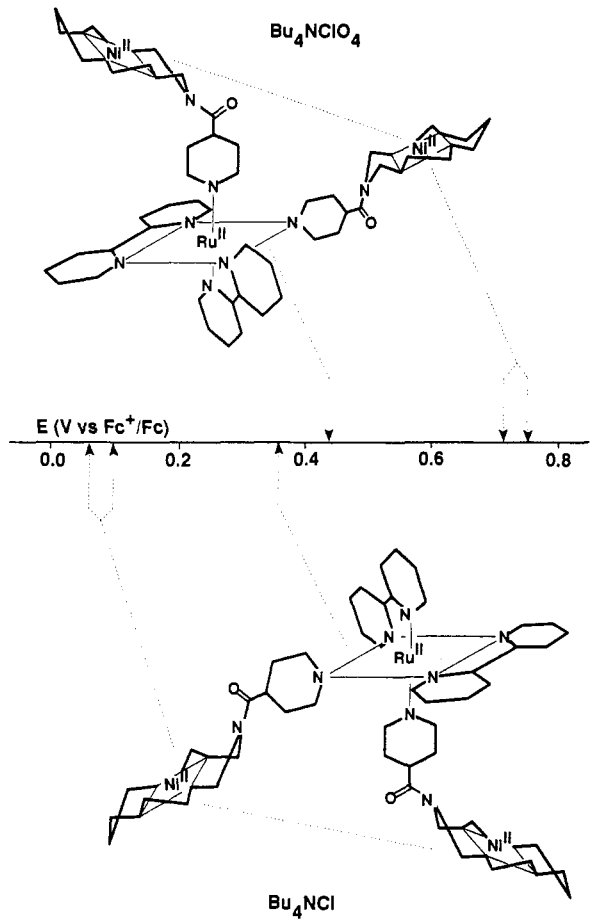

Figure 3. Potential diagram illustrating the redox behavior of *cis*-$[Ru^{II}(bipy)_2(\mathbf{4b})_2]^{6+}$ in an MeCN solution. $E_{1/2}$ values in the upper part of the diagram refer to a solution 0.1 mol dm^{-3} in Bu_4NClO_4; $E_{1/2}$ values in the lower part refer to a solution 0.1 mol dm^{-3} in Bu_3BzCl.

Thus, the *cis*-$[Ru^{II}(bipy)_2Cl_2]$ complex has been reacted with 2 equiv of the functionalized ligand $\mathbf{4a}(ClO_4)_2\cdot HClO_4$ and $\mathbf{4b}(ClO_4)_2\cdot HClO_4$ to form the *cis*-$[Ru^{II}(bipy)_2(\mathbf{4a})_2]^{6+}$ and *cis*-$[Ru^{II}(bipy)_2(\mathbf{4b})_2]^{6+}$ supercomplexes, precipitated as the hexaperchlorate salts.

It should be noted that the *cis*-$[Ru^{II}(bipy)_2(\mathbf{4x})_2]^{6+}$ species (**x** = **a**, **b**) is very similar to the *cis*-$[Pt^{II}(\mathbf{4x})_2Cl_2]^{4+}$ supercomplex described in the previous section, in that it contains two metallocyclam subunits bound, through a pyridine fragment, to the adjacent corners of a square. However, as the $Ru^{II}N_6$ moiety is typically redox active, through the Ru^{II}/Ru^{III} change, the metal center does not exert in this case a merely structural role but further contributes to the redox activity of the supercomplex.

The differential pulse voltammetry investigation on a MeCN solution 0.1 mol dm^{-3} in Bu_4NClO_4 and 10^{-3} mol dm^{-3} in *cis*-$[Ru^{II}(bipy)_2(\mathbf{4b})_2](ClO_4)_6$ showed two reversible peaks of different intensity, in the oxidation scan. Controlled potential electrolysis experiments indicated a one-electron consumption for the less anodic peak and the consumption of two electrons for the more anodic one. Thus, the first oxidation process has to be ascribed to the Ru^{II}/Ru^{III} change and the second one to the two-electron oxidation of the two metallocyclam subunits. The 90-mV half-height width of the more anodic DPV peak indicated that the two-electron process is statistically controlled ($\Delta E = 36$ mV) and that the two appended macrocyclic subunits display a completely independent redox activity. The sequence of the corresponding potential values is illustrated in the unidimensional diagram in Figure 3.

If $BzBu_3NCl$ is used as a background electrolyte, instead of Bu_4NClO_4, a drastic change in the voltammetric response of the *cis*-$[Ru^{II}(bipy)_2(\mathbf{4b})_2]^{6+}$ supercomplex is observed; also in this

(23) Colamarino, P.; Orioli, P. L. *J. Chem. Soc., Dalton Trans.* **1975**, 1656 and references therein.
(24) Richardson, D. E.; Taube, H. *Inorg. Chem.* **1981**, *20*, 1278.
(25) Krause, R. A. *Inorg. Chim. Acta* **1977**, *22*, 209.

case, two peaks are observed on the oxidation scan, in the DPV investigation. However, controlled potential electrolysis experiments assigned the less anodic peak to a two-electron process and the more anodic peak to a one-electron oxidation process: the reverse sequence compared to the case for the Bu_4NClO_4 solution! In particular, the two-electron wave becomes less anodic than the one-electron wave (see the potential values in the lower part of the diagram in Figure 3). This effect seems to be connected with the different stabilizing effect exerted by Cl^- ions on the Ru^{III} and Ni^{III} centers. In particular, the oxidation of the Ni^{II} tetraaza macrocyclic fragment involves the formation of a trans-octahedral complex (d^7, low-spin), in which the two axial positions are occupied by solvent molecules or by anions. Whereas the poorly coordinating ClO_4^- ions can hardly compete with the solvent molecules for the axial coordination sites, the strongly ligating Cl^- ions definitively occupy the apices of the elongated octahedron and stabilize the trivalent state.[26] Therefore, replacing of ClO_4^- by Cl^- as an anion of the supporting electrolyte causes a dramatic decrease of the $E_{1/2}$ value: more than 0.6 V! Such a stabilizing effect is not expected for the coordinatively saturated $Ru^{II}N_6$ subunit. Indeed, a very moderate potential decrease is observed also in the case of the Ru^{II}/Ru^{III} redox change (0.1 V). It should be noted that the sp^2 nitrogen atoms of 2,2'-bipyridine and of the functionalized pyridine molecules are so firmly bound to the Ru center that they cannot be replaced by any anion, under the conditions of the electrochemical investigation. However, it should be considered that anions present in solution of a not too polar solvent as MeCN can interact electrostatically with the RuN_6 moiety, in the form of an ion pair. Thus, the moderate stabilization of the Ru^{III} state may reflect the formation of tighter ion pairs with Cl^- ions, compared to ClO_4^- ions, which present a much lower charge density.

In any case, the *cis*-$[Ru^{II}(bipy)_2(\mathbf{4b})_2]^{6+}$ species represents an unprecedented example of a coordination compound displaying three-electron redox activity, in which the mode of the electron release, (1 + 2) or (2 + 1), can be switched by varying the nature of the background electrolyte.

(26) Haines, R. I.; McAuley, A. *Coord. Chem. Rev.* **1982**, *39*, 77.

Conclusions

Coordination chemists have produced, during the last century or so, hundreds of metal-centered systems, redox active through a one-electron redox change, whose electrode potential can be conveniently modulated by making synthetic modifications on the coordinating framework. More sophisticated systems able to exchange a wanted number of electrons, according to a predetermined sequence, at desired values of potential can be now prepared, following the principles of *supramolecular chemistry*. Moreover, the use of metal centers as structural elements allows one to control quite easily the topology of the multielectron redox systems, allowing one to place the redox sites in chosen positions, at predetermined distances. For instance, in the cases discussed before, the employed structural metal centers, $>Pt^{II}Cl_2$ and $>Ru^{II}(bpy)_2$, allowed the placement of two equivalent redox-active fragments in the adjacent corners of a square. The use of further metal centers may allow the design of multisite redox systems of varying topologies, which are related to the type of coordination polyhedron which has been chosen. In this sense, the *coordinative* approach seems much more versatile and promising than the *covalent* one, as far as the design of multielectron redox systems is concerned.

Acknowledgment. This work was supported by grants from the National Council of Research (CNR, Rome) and from the Ministry of the University (MURST, Rome). A.D.B. is indebted to the Xunta de Galicia for a research fellowship.

Supplementary Material Available: Tables of anisotropic thermal parameters for the non-hydrogen atoms, fractional atomic coordinates and isotropic thermal parameters, and complete bond distances and angles (Tables V–VII) (5 pages). Ordering information is given on any current masthead page.